

RESEARCH ARTICLE

Hamiltonian replica-exchange in GROMACS:
a flexible implementation

Giovanni Bussi

*Scuola Internazionale Superiore di Studi Avanzati (SISSA),
via Bonomea 265, 34136 Trieste, Italy**(April 30, 2013)*

A simple and general implementation of Hamiltonian replica exchange for the popular molecular-dynamics software GROMACS is presented. In this implementation, arbitrarily different Hamiltonians can be used for the different replicas without incurring in any significant performance penalty. The implementation was validated on a simple toy model - alanine dipeptide in water - and applied to study the rearrangement of an RNA tetraloop, where it was used to compare recently proposed force-field corrections.

Keywords: Hamiltonian replica exchange; solute tempering; RNA tetraloop

1. Introduction

Molecular dynamics (MD) is a powerful tool which can be used to simulate the time evolution of molecular systems with great accuracy. However, its application to realistic problems suffers from the so-called time-scale issue. Indeed, whereas typical trajectories simulated with empirical force fields are nowadays on the order of $1 \mu\text{s}$ long, interesting events such as phase transitions, chemical reactions and conformational changes often need much longer time scales. In spite of the development of fast and scalable MD software [see, e.g., 1] and *ad hoc* hardware [see, e.g., 2], many interesting problems can be expected to remain unaffordable with direct MD simulations for several decades. This issue has pushed the development of many techniques that allow to effectively accelerate MD so as to be able to study relevant problems with relatively low computational effort. A class of methods is based on the idea of choosing *a priori* a small set of collective variables which are then biased during the simulation (e.g. umbrella sampling [3] and metadynamics [4]). A common problem with these techniques is that their efficiency and accuracy is determined by the choice of the collective variables, which is often a difficult task. Another class of methods is based on the idea of raising temperature so as to accelerate sampling (e.g. simulated tempering [5] and parallel tempering [6, 7]). In parallel tempering several replicas of the same system are simulated at different temperature, and coordinates are exchanged from time to time with a Monte Carlo procedure. A very well known issue of parallel tempering is that the number of replicas required to span a preassigned temperature range grows with the system size. More generally, all these temperature-based methods suffer from the fact

*Corresponding author. Email: bussi@sissa.it

that the entire system under investigation is accelerated. Thus, while they do not require any *a priori* knowledge of the investigated events and can be often used blindly, they also do not allow the user to embed any knowledge about the problem in the simulation setup. Hamiltonian replica-exchange (HREX) methods [8], where different replicas evolve according to different Hamiltonians, are in a sort of intermediate position among the two mentioned classes of methods, and thus provide an interesting compromise among them. On the one hand, they are simpler to use when compared with collective-variable based methods. Indeed, dependence of the results on the choice of the modified Hamiltonian is smaller than dependence of, say, umbrella sampling efficiency on the choice of the collective variables. On the other hand, they are more efficient than parallel tempering because the number of required replicas is typically much less. A wealth of recipes for HREX has been proposed in the last years [see, among others, 8–21].

We here focus on one of the most successful among these recipes, namely replica-exchange solute tempering in its REST2 variant [20], and discuss an implementation of this method in the popular MD software GROMACS [1]. We also discuss a possible extension of REST2 where only a part of the solute is modulated. The implementation is validated on alanine dipeptide in water and applied to study the stability of an RNA tetraloop, comparing two recently developed force fields [22, 23].

2. Methods

2.1. Hamiltonian replica exchange

We consider a system with coordinates r and subject to a potential energy $U(r)$. We assume that the potential is built as a sum of few-body terms as it is conventionally done for the atomistic modeling of biomolecules [24, 25], although the method can be easily generalized to other force fields. The system is assumed to be coupled with a thermal bath at temperature T so that the probability of exploring a configuration is $P(r) \propto e^{-\frac{U(r)}{k_B T}}$ where k_B is the Boltzmann constant. Replica exchange methods are generally based on the idea of sampling one “cold” replica, from which the unbiased statistics can be extracted, plus a number of “hot” replicas, whose only purpose is that of accelerating sampling. The “hottest” replica should explore the space fast enough to overcome barriers for the process under investigation, whereas the intermediate replicas are necessarily introduced to bring the system smoothly from the “hottest” ensemble to the “coldest” ensemble. Indeed, the number of needed replicas is actually related to the difference between the hottest and the coldest ensembles. In plain parallel tempering “hot” and “cold” refers to physical temperature as controlled by a thermostat, whereas in the general Hamiltonian replica exchange “hot” replicas can be biased in an arbitrary manner so as to accelerate sampling. It should be noted that transition rates for processes which are hindered by entropic barriers are not necessarily expected to increase with temperature, so that the efficiency of parallel tempering in those cases could be lower [26].

In the most general formulation, each replica is simulated at a different temperature and using a different Hamiltonian. Calling r_i the coordinate of the i -th replica and N the number of replicas, the resulting product ensemble is

$$P(r_1) \times \cdots \times P(r_N) \propto e^{-\frac{U_1(r_1)}{k_B T_1} - \cdots - \frac{U_N(r_N)}{k_B T_N}}$$

If $U_1 = U_2 = \cdots = U_N$, plain parallel tempering is recovered. Since the ensemble

probability only depends on $U/(k_B T)$, a double temperature is completely equivalent to a halved energy. The advantage of scaling the potential energy instead of the temperature is related to the fact that the energy is an extensive property, whereas the temperature is an intensive one. One can thus selectively choose a portion of the system and specific parts of the Hamiltonian to be “heated.” Still there is some arbitrariness in the scaling of the coupling terms. In our approach, we split the system in two regions \mathcal{H} (hot) and \mathcal{C} (cold) so that each atom is statically assigned to either the \mathcal{H} or the \mathcal{C} region, and defined a parametrized Hamiltonian which depends on λ as follows:

- The charge of atoms in the \mathcal{H} region is scaled by a factor $\sqrt{\lambda}$.
- The ϵ (Lennard-Jones parameter) of atoms in the \mathcal{H} region is scaled by a factor λ .
- The proper dihedral potentials for which the first *and* fourth atoms are in the \mathcal{H} region is scaled by a factor λ .
- The proper dihedral potentials for which either the first *or* the fourth atom is in the \mathcal{H} region is scaled by a factor $\sqrt{\lambda}$.

With this choice, only force-field terms contributing to energy barriers, i.e. electrostatic, Lennard-Jones and proper dihedrals, are scaled in such a manner that:

- Interactions inside the the \mathcal{H} region are kept at an effective temperature T/λ .
- Interactions between the \mathcal{H} and the \mathcal{C} regions are kept at an effective intermediate temperature $T/\sqrt{\lambda}$.
- All interactions inside the \mathcal{C} region are kept at temperature T .

We underline that the effective temperature is not induced by a thermostat and that the simulations as well as the exchanges among replicas are performed at thermodynamics equilibrium. The scaling parameter λ can be chosen to be any real number between 1, for the reference, unmodified system, and 0. The latter value corresponds to no interaction in the \mathcal{H} region or, equivalently, to infinite temperature. Albeit the code allows choosing $\lambda = 0$ (infinite temperature), this is usually not an optimal choice because it would lead to a very low acceptance rate. We also notice that if the \mathcal{H} region has a net charge, the “hot” replicas will also have a total charge which is different from that of the unbiased replica. This is not a problem because in periodic calculations based on Ewald-like methods [27] a neutralizing background is implicitly added. As a final observation, our choice for the treatment of scaling parameters for dihedrals leads to a consistent scaling of dihedral potentials and corresponding 1-4 interactions.

When used for the entire solute, our implementation exactly reproduces REST2 [20]. Moreover, it was constructed in such a manner to be used in a partial tempering scheme, where only a portion of the solute is heated. It is straightforward to extend the formulation so as to simulate replicas at different pressures [28].

2.2. Implementation details

We implemented our replica exchange methodology in GROMACS 4.6.1 [1] patched with the PLUMED plugin [29], version 2.0b0. The combination of GROMACS and PLUMED was used to allow HREX and enhanced sampling methods based on biasing *a priori* chosen collective variables to be used simultaneously. To increase the flexibility of the method, we coded it in such a manner that independent topology files can be used for different replicas. In principle, different PLUMED input files could also be used, thus adding different bias potentials or restraints on the different replicas, albeit we did not exploit this feature here.

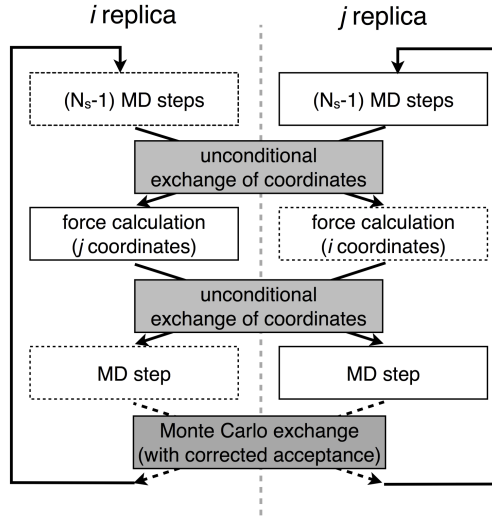


Figure 1. Flowchart of our Hamiltonian replica exchange implementation. After having performed $N_s - 1$ molecular dynamics steps, a coordinate swap is performed. Then, the energy is recomputed and coordinates are swapped again. At this point a further MD step is done and a real exchange is attempted with a corrected Monte Carlo acceptance [Equation (1)].

The flow of the modified replica exchange is depicted in Figure 1. At the beginning of a timestep where an exchange is required an exchange is unconditionally performed and the total energy is computed using the local force field for the coordinates obtained from another processor. This energy is stored for later usage, and original (unswapped) coordinates are restored with an extra unconditional exchange. At the end of the MD step, when the actual exchange is attempted, the previously stored energy is used to accept/reject the exchange. The acceptance is then computed in the most general manner, which allows replicas with different bias potential, Hamiltonian and temperature

$$\alpha = \min \left(1, e^{\frac{-\bar{U}_i(r_j) + \bar{U}_i(r_i)}{k_B T_i} + \frac{-\bar{U}_j(r_i) + \bar{U}_j(r_j)}{k_B T_j}} \right) \quad (1)$$

where \bar{U} is defined as the sum of the force-field potential and possibly additional potentials as computed by PLUMED. Force-field parameters for the “hot” replicas are edited using simple scripts. In spite of the two extra swaps required at each attempted exchange, the overhead is rather low. Its exact value depends on the attempt frequency for replica exchange, and in our experience never exceeded 10%.

We observe that our implementation differs from the one proposed in Ref. [19], where the free-energy perturbation method already available in GROMACS has been exploited. Because of the way interactions for $0 < \lambda < 1$ are treated in GROMACS, strictly speaking it is not possible to set up a simulation following REST2 prescriptions using free-energy perturbation. Moreover, calculation of non-bonded interactions in the free-energy perturbation are slower in GROMACS, and can introduce significant overhead even in the plain MD which is performed between exchanges. On the other hand, the overhead of our implementation is limited to the exchange step. Since the stride between exchanges is typically on the order of at least 100 steps, this overhead is negligible.

3. Applications

3.1. Solute tempering: alanine dipeptide

As a first test case we focused on alanine dipeptide, a standard benchmark for enhanced-sampling methods. The low-energy conformations of this system can be described using the two dihedral angles of the Ramachandran plot, ϕ and ψ . Transitions between conformations C_{7eq} ($\phi = -80^\circ, \psi = 75^\circ$) and C_{7ax} ($\phi = 75^\circ, \psi = -75^\circ$) are hindered by large free-energy barriers. An alanine dipeptide molecule modeled with Amber99sb force-field [30] was solvated in a box containing approximately 700 TIP3P water molecules [31]. All bonds were kept rigid [32, 33], and equations of motion were integrated using a timestep of 2fs. Long-range electrostatics was treated using particle-mesh Ewald [34], and temperature was controlled by stochastic velocity rescaling [35].

We performed a REST2 [20] simulation using 5 replicas with values of λ ranging from 1 to 0.3 following a geometric distribution. This choice lead to an acceptance rate ranging from 35% to 50%. Exchanges are attempted every 100 steps. In Figure 2 the distributions of ψ and ϕ angles explored by the first and last replica are shown. It can be seen how the change in the Hamiltonian effectively raises the temperature of the molecule, thus decreasing the impact of free-energy barriers. The time series of the ϕ dihedral angle in the replica with $\lambda = 1$ is shown in Figure 3, together with a much longer single-replica simulation. At the price of a factor 5 in the computational cost, the HREX simulation sampled the phase space much faster. Since several transitions between C_{7eq} and C_{7ax} are observed, we could compute the relative stability of the two metastable minima, which converged quickly (Figure 3c). The free-energy profile as a function of the ϕ dihedral angle was also computed and compared with a reference free-energy landscape obtained using well-tempered metadynamics [36] (well-tempered factor $\Delta T=2100K$, initial deposition rate $\omega=6.25$ kJ/mol/ps, Gaussian width $\sigma = 20^\circ$, simulation length 10ns). Profiles obtained at different stages of the HREX simulation and reference metadynamics results are shown in Figure 3d. For this simple system, metadynamics has the advantage of providing good statistics also on the free-energy barriers. However, HREX is capable of reproducing the correct free-energy difference between the two minima and the correct shape of the two free-energy wells using a minimal information about the simulated system. This can be an advantage in cases where choosing collective variables is more difficult, such as the one discussed below.

3.2. Partial tempering: RNA tetraloop

The second application is the structural characterization of a UUCG RNA tetraloop. UUCG tetraloops and small RNA hairpins have been characterized *in vitro* and *in silico* by several groups [37–41]. Atomistic molecular simulations of tetraloop folding are difficult because of slow sampling and of the well-known inaccuracies of classical force fields for RNA [40]. In a recent paper, Kurova *et al.* [41] have shown the results of a long parallel-tempering simulation of a UUCG tetraloop. In their work, the full hairpin is initialized in a straight conformation, so as to blindly predict its folded structure and stability. Our investigation was instead limited to the exploration of the conformational space available for the tetraloop, without studying the full hairpin formation.

We started from an experimental structure (residue 31-38 of PDB 1F7Y [43], sequence GCUUCGGC) solvated in a box containing approximately 4600 water molecules and added 14 Na^+ and 7 Cl^- atoms. All other simulation details were chosen as in Subsection 3.1. After equilibration, we restrained the 6 Watson-Crick

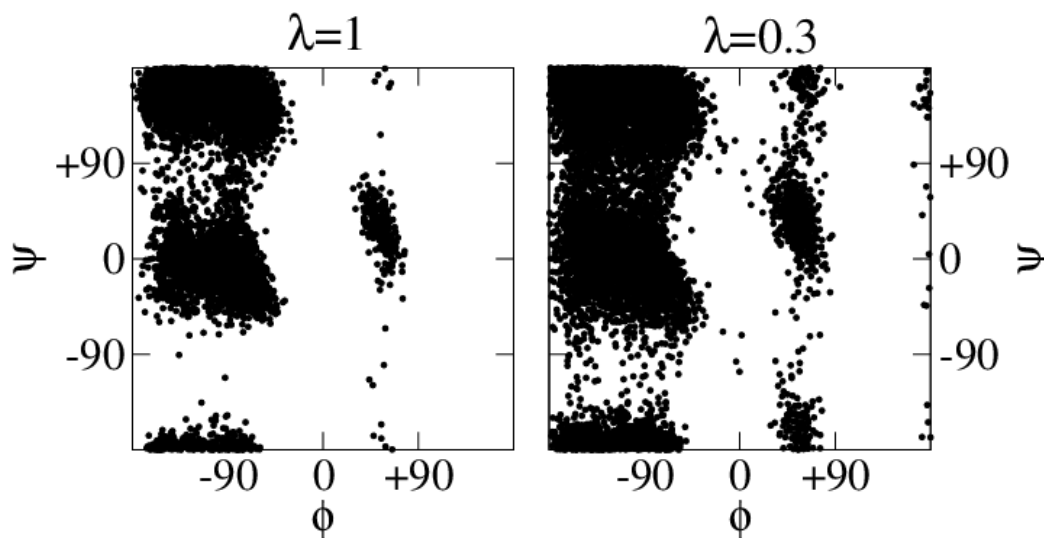


Figure 2. Conformational space explored for alanine dipeptide by first ($\lambda = 1$, left) and last ($\lambda = 0.3$, right) replica. It can be seen that the conformational space explored by last replica is larger.

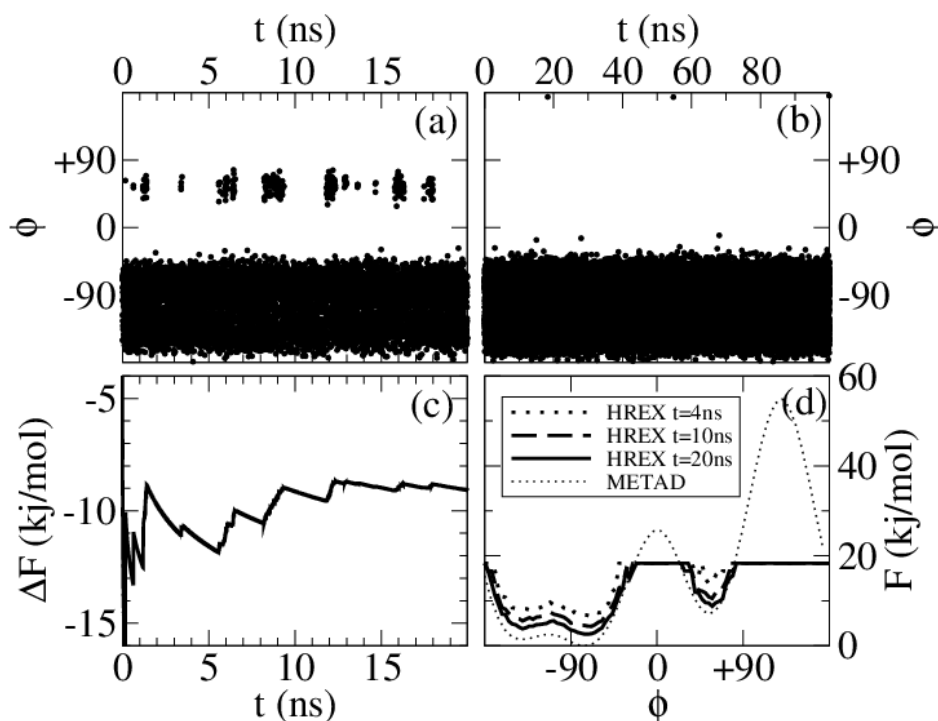


Figure 3. Convergence of Hamiltonian replica exchange (HREX) for alanine dipeptide. ϕ angle for (a) replica at $\lambda = 1$ and (b) for a longer, serial simulation. (c) Estimate of the free-energy difference between C_{7eq} and C_{7ax} as a function of the simulated time per replica, obtained from analyzing the replica at $\lambda = 1$. (d) Free-energy landscape as a function of dihedral angle ϕ , as obtained from HREX, compared with a reference metadynamics calculation. Results for HREX are shown for different simulation lengths (simulated time per replica equal to 4, 10 and 20 ns, as indicated), whereas metadynamics profile has been obtained from a single 10 ns simulation.

hydrogen bonds of the stem (enforced distance 3\AA , stiffness 25 kJ/mol/\AA^2 ; see Figure 4) so as to suppress fraying of the first base pair and avoid severe unfolding of the hairpin. We selected as a “hot” region the 4 nucleotides corresponding to the tetraloop (see Figure 4), leaving the Hamiltonian for the stem unbiased in all the replicas. We simulated 16 replicas using values of λ ranging from 1 to 0.3 with a geometric distribution, leading to an acceptance rate which is between 30% and 50%. This protocol allowed us to accelerate the sampling of different

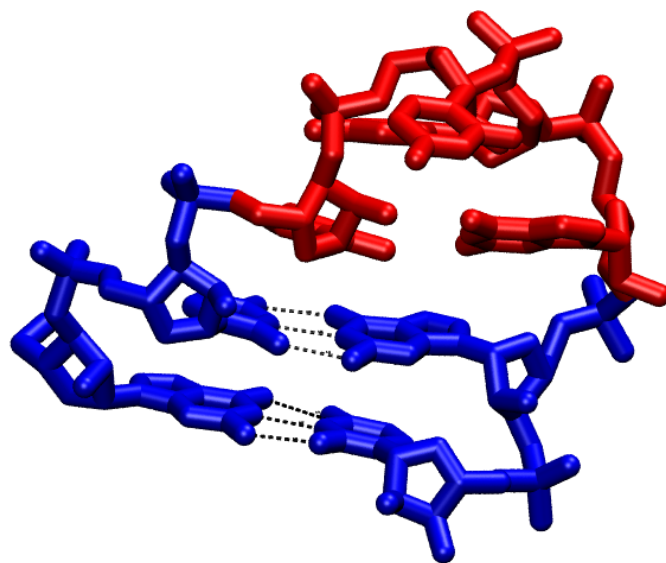


Figure 4. Representation of the RNA tetraloop, hydrogen atoms not shown. Atoms in the “hot” region (tetraloop) are shown in red. Atoms in the “cold” region (stem) are shown in blue. Restrained Watson-Crick hydrogen bonds are also marked. Graphics made with VMD [42].

conformations of the tetraloop, without perturbing too much the stem. Simulations were performed using two recently developed force fields, both based on Amber99 force field [25]: parmbsc0 force field [22] (from now on, bsc0) and ff99bsc0_χOL3 force field [23] (from now on, bsc0-OL).

In Figure 5 the root-mean-square deviation (RMSD) of stem and loop from the reference experimental structure is shown. The simulation performed using the bsc0 force-field quickly interconverted into an artificial “ladder-like” structure [44] for which the RMSD of the stem from the experimental structure is $\approx 4\text{\AA}$. This is a known problem of the bsc0 force field, and has been already detected by means of long MD simulations [see 40, and references therein]. Notably, with Hamiltonian replica exchange this happened in a very short time ($\approx 1\text{ ns}$ per replica). The coexistence of a correct (low RMSD) and artificial (high RMSD) structure in the Figure 5a is due to the fact that the only the replica at $\lambda = 1$ is shown. More precisely, some trajectories switched to the “ladder-like” structure, and other ones did not, resulting in a mixed ensemble for the $\lambda = 1$ replica. The native loop structure was even less stable: After approximately 10 ns per replica the native structure was destroyed in all replicas and completely disappeared from the explored ensemble (Figure 5b). On the other hand, the simulation performed using the bsc0-OL force field behaved in a qualitatively better way. The stem was very stable on the same timescale (Figure 5c), and, even if spurious structures were appearing in the loop, the native structure was still populated after 15 ns per replica (Figure 5d). This indicates that the actually explored ensemble and the experimental one are reasonably overlapping.

These results show that Hamiltonian replica exchange, especially in variants where only a portion of a larger molecule is biased, can be very effective in accelerating conformational sampling. In particular, we were able to detect the known problems of the bsc0 force field in a short computational time. A deeper investigation of the force-field dependence of the conformational space available for an RNA tetraloop will be the subject of further investigations.

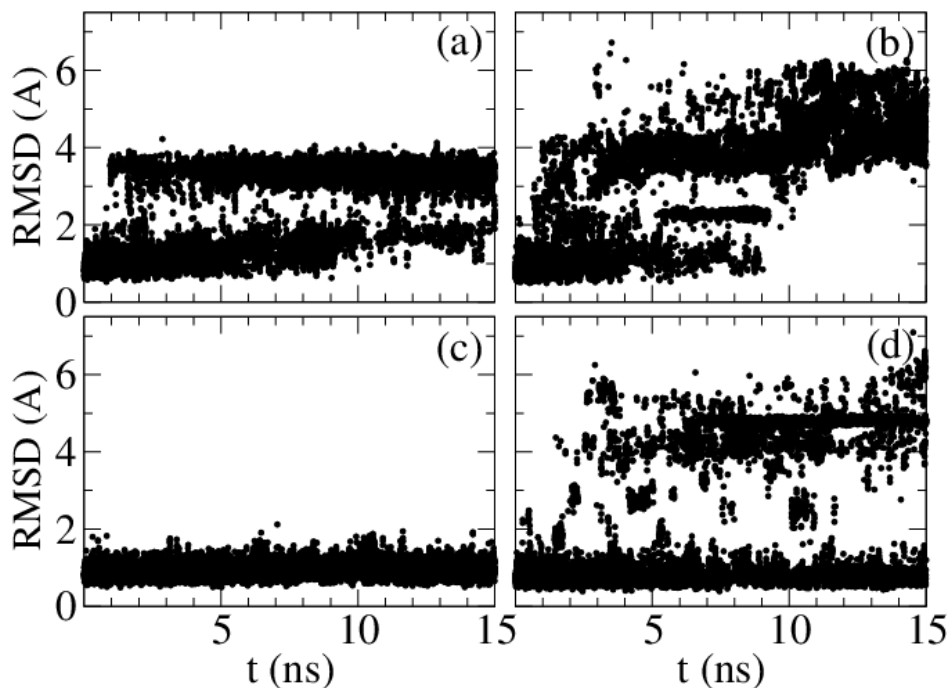


Figure 5. Root-mean-square deviation of hairpin stem (bases 1, 2, 7 and 8) and loop (bases 3, 4, 5, 6) from the experimental structure, as obtained from the unbiased replica ($\lambda = 1$) as a function of simulation time per replica. Simulations were performed using bsc0 force field [stem (a) and loop (b)] and bsc0-OL force field [stem (c) and loop (d)]. It can be seen that the latter force field better stabilizes the native structure for the stem. Loop stability is also improved with bsc0-OL, but in this case also non-native, high RMSD, structures are sampled.

4. Conclusions

In conclusion, a flexible implementation of Hamiltonian replica exchange for GROMACS was discussed. This implementation can be used to combine replicas at different temperature, pressure, and using different force-fields. It was validated on the simple case of alanine dipeptide in water, where results obtained with a reference well-tempered metadynamics calculation were correctly reproduced. Then, Hamiltonian replica exchange was used to extensively sample the available conformations in an RNA tetraloop, comparing two different force fields. Our software is available upon request and will be distributed together with the next release of PLUMED.

Acknowledgments

The research leading to these results has received funding from the European Research Council under the European Union’s Seventh Framework Programme (FP/2007-2013) / ERC Grant Agreement n. 306662, S-RNA-S. Simulations were performed partly on local machines and partly at the CINECA supercomputing center. The ISCRA grant HP10B194XL and the IIT Platform “Computation” are acknowledged for the availability of high performance computing resources. Sandro Bottaro and Maria Darvas are acknowledged for providing a port of the bsc0-OL force field for GROMACS. Sandro Bottaro is also acknowledged for carefully reading the manuscript. Luca Bellucci and Ben Cossins are acknowledged for testing preliminary versions of this replica-exchange implementation.

References

- [1] B. Hess, C. Kutzner, D. Van Der Spoel and E. Lindahl, *J. Chem. Theory Comput.* **4** (3), 435 (2008).
- [2] D.E. Shaw, P. Maragakis, K. Lindorff-Larsen, S. Piana, R.O. Dror, M.P. Eastwood, J.A. Bank, J.M. Jumper, J.K. Salmon, Y. Shan *et al.*, *Science* **330** (6002), 341 (2010).
- [3] G.M. Torrie and J.P. Valleau, *J. Comput. Phys.* **23** (2), 187 (1977).
- [4] A. Laio and M. Parrinello, *Proc. Natl. Acad. Sci. U.S.A.* **99** (20), 12562 (2002).
- [5] E. Marinari and G. Parisi, *Europhys. Lett* **19** (6), 451 (1992).
- [6] U.H.E. Hansmann, *Chem. Phys. Lett.* **281** (1–3), 140 (1997).
- [7] Y. Sugita and Y. Okamoto, *Chem. Phys. Lett.* **314** (1–2), 141 (1999).
- [8] Y. Sugita and Y. Okamoto, *Chem. Phys. Lett.* **329** (3–4), 261 (2000).
- [9] H. Fukunishi, O. Watanabe and S. Takada, *J. Chem. Phys.* **116**, 9058 (2002).
- [10] P. Liu, B. Kim, R.A. Friesner and B.J. Berne, *Proc. Natl. Acad. Sci. U.S.A.* **102** (39), 13749 (2005).
- [11] R. Affentranger, I. Tavernelli and E. Di Iorio, *J. Chem. Theory Comput.* **2** (2), 217 (2006).
- [12] M. Fajer, D. Hamelberg and J. McCammon, *J. Chem. Theory Comput.* **4** (10), 1565 (2008).
- [13] C. Xu, J. Wang and H. Liu, *J. Chem. Theory Comput.* **4** (8), 1348 (2008).
- [14] M. Zacharias, *J. Chem. Theory Comput.* **4** (3), 477 (2008).
- [15] J. Vreede, M.G. Wolf, S.W. de Leeuw and P.G. Bolhuis, *J. Phys. Chem. B* **113**, 6484 (2009).
- [16] S.G. Itoh, H. Okumura and Y. Okamoto, *J. Chem. Phys.* **132**, 134105 (2010).
- [17] M.S. Lee and M.A. Olson, *J. Chem. Theory Comput.* **6** (8), 2477 (2010).
- [18] Y. Meng and A. Roitberg, *J. Chem. Theory Comput.* **6** (4), 1401 (2010).
- [19] T. Terakawa, T. Kameda and S. Takada, *J. Comput. Chem.* **32** (7), 1228 (2011).
- [20] L. Wang, R. Friesner and B. Berne, *J. Phys. Chem. B* **115** (30), 9431 (2011).
- [21] C. Zhang and J. Ma, *Proc. Natl. Acad. Sci. U.S.A.* **109** (21), 8139 (2012).
- [22] A. Pérez, I. Marchán, D. Svozil, J. Sponer, T. Cheatham III, C. Loughton and M. Orozco, *Biophys. J.* **92** (11), 3817 (2007).
- [23] M. Zgarbova, M. Otyepka, J. Sponer, A. Mladek, P. Banas, T.E. Cheatham and P. Jurecka, *J. Chem. Theory Comput.* **7** (9), 2886 (2011).
- [24] W. Cornell, P. Cieplak, C. Bayly, I. Gould, K. Merz, D. Ferguson, D. Spellmeyer, T. Fox, J. Caldwell and P. Kollman, *J. Am. Chem. Soc.* **117** (19), 5179 (1995).
- [25] T. Cheatham 3rd, P. Cieplak and P. Kollman, *J. Biomol. Struct. Dyn.* **16** (4), 845 (1999).
- [26] H. Nymeyer, *J. Chem. Theory Comput.* **4** (4), 626 (2008).
- [27] T. Darden, D. York and L. Pedersen, *J. Chem. Phys.* **98** (12), 10089 (1993).
- [28] T. Okabe, M. Kawata, Y. Okamoto and M. Mikami, *Chem. Phys. Lett.* **335** (5–6), 435 (2001).
- [29] M. Bonomi, D. Branduardi, G. Bussi, C. Camilloni, D. Provasi, P. Raiteri, D. Donadio, F. Marinelli, F. Pietrucci, R. Broglia and M. Parrinello, *Comput. Phys. Commun.* **180** (10), 1961 (2009).
- [30] K. Lindorff-Larsen, S. Piana, K. Palmo, P. Maragakis, J.L. Klepeis, R.O. Dror and D.E. Shaw, *Proteins: Struct., Funct., Bioinf.* **78** (8), 1950 (2010).
- [31] W.L. Jorgensen, J. Chandrasekhar, J.F. Madura, R.W. Impey and M.L. Klein, *J. Chem. Phys.* **79**, 926 (1983).
- [32] S. Miyamoto and P. Kollman, *J. Comput. Chem.* **13** (8), 952 (1992).
- [33] B. Hess, H. Bekker, H.J.C. Berendsen and J.G.E.M. Fraaije, *J. Comp. Chem.* **18**, 1463 (1997).
- [34] U. Essmann, L. Perera, M. Berkowitz, T. Darden, H. Lee and L. Pedersen, *J. Chem. Phys.* **103** (19), 8577 (1995).
- [35] G. Bussi, D. Donadio and M. Parrinello, *J. Chem. Phys.* **126** (1), 014101 (2007).
- [36] A. Barducci, G. Bussi and M. Parrinello, *Phys. Rev. Lett.* **100** (2), 020603 (2008).
- [37] H. Ma, D.J. Proctor, E. Kierzek, R. Kierzek, P.C. Bevilacqua and M. Gruebele, *J. Am. Chem. Soc.* **128** (5), 1523 (2006).
- [38] A.E. Garcia and D. Paschek, *J. Am. Chem. Soc.* **130** (3), 815 (2008).
- [39] G. Zuo, W. Li, J. Zhang, J. Wang and W. Wang, *J. Phys. Chem. B* **114** (17), 5835 (2010).
- [40] P. Banas, D. Hollas, M. Zgarbova, P. Jurecka, M. Orozco, T.E. Cheatham, J. Sponer and M. Otyepka, *J. Chem. Theory Comput.* **6** (12), 3836 (2010).
- [41] P. Kuhrova, P. Banas, R.B. Best, J. Sponer and M. Otyepka, *J. Chem. Theory Comput.* **9** (4), 2115 (2013).
- [42] W. Humphrey, A. Dalke and K. Schulten, *J. Mol. Graph.* **14** (1), 33 (1996).
- [43] E. Ennifar, A. Nikulin, S. Tishchenko, A. Serganov, N. Nevskaya, M. Garber, B. Ehresmann, C. Ehresmann, S. Nikonov and P. Dumas, *J. Mol. Biol.* **304** (1), 35 (2000).
- [44] V. Mlynsky, P. Bans, D. Hollas, K. Réblová, N.G. Walter, J. Sponer and M. Otyepka, *The Journal of Physical Chemistry B* **114** (19), 6642 (2010).